PHASE-SENSITIVE CELLULAR AUTOMATA ON STOCHASTIC NETWORK AS A MODEL FOR CARDIAC PACEMAKER RHYTHMICITY*

Danuta Makowiec

Institute of Theoretical Physics and Astrophysics, University of Gdańsk
Wita Stwosza 57, 80-952 Gdańsk, Poland
fizdm@univ.gda.pl

(Received December 5, 2011)

Oscillating cellular automata placed on two-dimensional stochastic lattice are proposed to model normal and abnormal cardiac pacemaker activity. In addition to Greenberg–Hasting approach, interactions which elongate the cellular period are proposed. Stationary states of the proposed system depend on density of intercellular connections, and thresholds for cell-to-cell interactions. The transition from expanding to collapsing wave patterns is observed at certain model parameters. A physiological meaning can be given to that transition, namely, as the arrhythmia phenomenon developing in the real heart due to abnormal high potassium concentration in the blood.

DOI:10.5506/APhysPolBSupp.5.85
PACS numbers: 87.19.Hh, 87.17.Aa, 87.18.Mp

1. Introduction

Networks containing many oscillating units appear in different fields of science. The sinoatrial nodal tissue — the first mammalian pacemaker — is one of such example. Mechanisms involved in the coordination of a large group of pacemaker cells have been discussed since 1980, see [1] for review. To this day, they are still not clear. Since the phenomenon of the phase sensitivity of pacemaker cells to discrete external stimuli is ubiquitous and universal in different species, therefore the hypothesis of a democratic consensus achieved through the mutual entrainment of cells has been proposed [2]. This hypothesis has been verified in experiments with cells from different mammalian pacemaker cells.

* Presented at the Summer Solstice 2011 International Conference on Discrete Models of Complex Systems, Turku, Finland, June 6–10, 2011.

Entrainment literally means to get aboard a train. However, in the case of interacting systems this notion is used to describe changes carried along by a train of controlling stimuli. In a system where each unit is both source and recipient of stimuli, like in the pacemaker tissue, the emergence of mutual entrainment is a sign of self-organization. Therefore, explaining the perpetual work of sinoatrial node (SAN) has become a challenging task for researchers working in the complex systems.

Much effort has been put to understand the collective dynamics of the oscillating units. If oscillators are identical, or are connected all-to-all, some mathematical analysis can be done [3]. However, real networks composed of real oscillators have often heterogeneous spatial structure and cellular oscillators are usually of many types. In order to model dynamics of such systems we must rely on simulation. Therefore, having little hope for rigorous approach, the stationary states obtained from simulations, we will call the solutions.

In the following, a cellular automata network will be proposed to study conditions when identical phase-sensitive oscillatory automata, called FRA cells, distributed in nodes of the stochastic 2-dim lattice, provide a robust oscillatory signal. The model of a pacemaker cell with the phase-sensitivity was introduced by Abramovich-Silvan *et al.* [5]. On the other hand, Greenberg and Hastings considered the simple discrete system — cellular automata, which reconstructed properties of the excitable tissue [6] in a critical but robust way [7]. The Greenberg–Hastings approach was successfully applied to model the chicken embryo heart [8]. Our proposition goes beyond the excitable tissue idea. We propose a new mechanism which enables to elongate the period of cellular oscillations.

The paper is organized as follows. In Sec. 2 we provide the physiological arguments supporting the presented approach. Then in Sec. 3 we give the formal definition of interactions and construct the network of intercellular connections. The results obtained by simulations are presented in Sec. 4. The effects of the self-organization are classified according to the type of patterns appearing in stationary states. The last section contains the discussion of the results with respect to the known physiology. The simplified FRA model, with interactions limited to period shortenings, is described in our earlier papers [9].

2. Physiological motivation for the FRA model

The sinus node tissue is flat, and its contents is usually described as rarely connected myocytes (*i.e.*, cardiac cells) [10, 11, 12, 13]. For example, in the canine tissue, each pacemaker cell is connected to 4, 5 or 6 spatially adjacent cells by the so-called gap junctions [14]. Cells transduce signals by these

connections. The pacemaker myocytes do not form any regular structure which is typical for myocytes in the atria or ventricles [12]. Moreover, the sinus node tissue is insulated from the atrium by collagen tissue. Therefore, the pacemaker can be reliably approximated by a square lattice with free boundary conditions where vertices are interpreted as myocytes, and where only some of lattice neighboring cells are interconnected [8].

There is a sequence of biochemical processes that changes the electrical potential of the membrane of myocyte, see Fig. 1 (a). This property can be observed on any myocyte. However, the course of the membrane potential in the pacemaker cell is substantially different from any atrial or ventricular cell. Firstly, the rapid increase of potential [marked as F in Fig. 1 (a)] is not as rapid as it develops in the atrial cell. The phenomenon of the rapid increase of the potential is called the action potential. After completing the action potential and reaching back to the lowest negative value, the membrane potential of a nodal cell does not stay resting, as it happens in the case of atrial cells, but continuously rises to the threshold value. Because of that, the pacemaker cells are self-excitatory, and therefore, we can approximate a pacemaker cell by an oscillating unit.

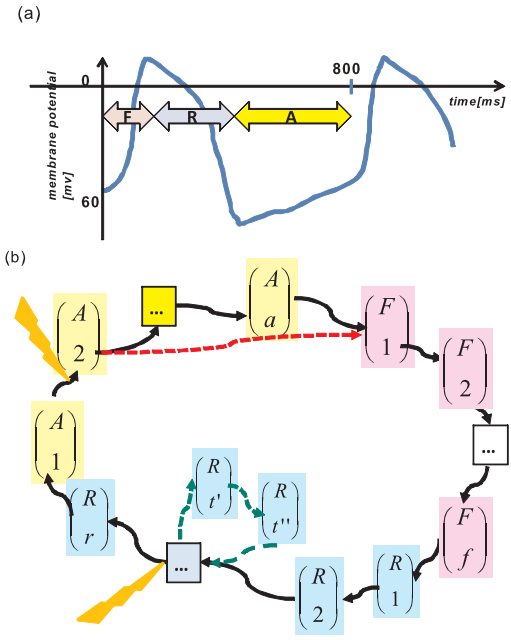

Fig. 1. (a) The course of the membrane potential of a sinus node cell (modified from [4]) and (b) illustration of a cycle of a FRA cell and its phasic sensitivity. Regular arrows describe unperturbed intrinsic cycle. Each wide arrow denotes an external stimulus which changes the cellular cycle. The corresponding changes are marked by dashed lines.

Plenty of ionic current models have been designed to describe the variety of electrophysiology of isolated cardiac cells, see [15] for a review. Numerical integrations of equations of these models can be challenging because of the differences in time and space scales [15]. The transition from systems describing interactions of few cells to significantly larger systems demands the coarse graining reduction. Therefore, the simplified approach, based on discrete state cellular automata should be particularly justified.

Let us design a cellular automaton for which the fast uprise of the membrane potential is represented by states denoted F_k which form the so-called called *Firing* phase, see Fig. 1 (b). After f steps in *Firing* phase a cell always moves to the phase called *Refractory*. The first *Refractory* state is denoted R_1. If the intrinsic cycle of a cell performs itself smoothly, *i.e.*, without interactions with the outside, then after r steps a cell becomes *Active* and its state is A_1. Finally, after a steps in *Active* phase a cell switches itself to F_1 state, *i.e.*, initiates the next action potential. However, if some external stimulus enter the cell when the cell is in A_k state then the next time step state is F_1. The cellular cycle is shortened. If an external stimulus occurs when the cell is in R_k state then the cell spends some extra time steps in the *Refractory* states. Therefore the cellular period is elongated.

3. Formal definitions of the FRA network

Def. of a FRA cell intrinsic cycle:
Let $\Sigma = \{F_k, R_k, A_k\}$, where $k \in \{1, 2, \ldots, n_\sigma\}$ and $n_\sigma \in \{f, r, a\}$ correspondingly, be the state space of a FRA cell.
Let $\phi(t)$ denote the phase of a FRA cell at time t.
Let $\phi(t) = \sigma_k$, where $\sigma_k \in \Sigma$ is any state of a FRA cell.
A cellular phase $\phi(t+1)$ in the next time step is

$$\begin{array}{ll} \phi(t+1) = \sigma_{k+1} & \text{if } k < n_\sigma \\ \phi(t+1) = \text{next}(\sigma)_1 & \text{if } k = n_\sigma \end{array} , \tag{1}$$

where $\text{next}(F) = R,\ \text{next}(R) = A,\ \text{next}(A) = F.$

Thus, a free evolution of FRA cell means cyclic repetitions of the following sequence of states:

$$F_1 F_2 \ldots F_f R_1, R_2 \ldots R_r A_1, A_2 \ldots A_a F_1 F_2 \ldots$$

which leads to oscillations with the so-called intrinsic cellular period: $T = f + r + a$.

Def. of FRA cell interactions:
If a FRA cell receives a stimulus then a cellular phase $\phi(t+1)$ in the next time step is:

$$\phi(t+1) = F_1 \quad \text{if} \quad \phi(t) = A_k, \text{ where } k = 1, \ldots, a\,, \tag{2}$$
$$\phi(t+1) = R_{\max\{1,g(k)\}} \quad \text{if} \quad \phi(t) = R_k, \text{ where } k = 1, \ldots, r\,, \tag{3}$$

where

$$g(k) = \lfloor k/2 \rfloor\,. \tag{4}$$

Rules (1) and (2) lead to the excitatory cellular automata studied by us earlier [9]. By adding rule (3), we assume that the cellular *Refractory* phase is rolled back by half time steps of the current advancement in the *Refractory* states if the cell receives a stimulus. Note that if $g(k) = k$ then we obtain the previous model.

In general, oscillations with periods other than T are imprints of interactions between cells. Let $T^* = f + r + 1$ denote the shortest possible cycle. It can occur if a stimulus is received just in the moment when a cell is in the first activity state A_1. To maintain such oscillations the stimulus with period T^* must act permanently. On the other hand, because of the rule (3), a cell is kept in *Refractory* phase as long as the stimulus is present. Therefore, there is no limit to the longest cycle.

In the case of interacting oscillating systems, the notion of the entrainment is often used to describe the process that leads to accepting the common period. In the simplified system — rules (1) and (2), the entrainment between FRA-type cells yielded the arrangement of cellular oscillatory phases what often effected in the emergence of spiral-wave patterns.

To learn more about the impact of rule (3) let us observe the entrainment in a system of two coupled FRA cells. Let us assume that each time a FRA cell is any F_k state, it sends a stimulus to a neighboring cell. We ask what kind of evolution is achieved if two FRA cells interact with each other.
The following cases should be considered:

— a cell in R_i meets a cell in F_j. Then

$$\begin{pmatrix} R_i \\ F_j \end{pmatrix} \to \begin{pmatrix} R_{i/2} \\ F_{j+1} \end{pmatrix} \to \ldots \begin{pmatrix} R_1 \\ R_1 \end{pmatrix}\,,$$

— a cell in A_i meets a cell in F_j. Then for some k

$$\begin{pmatrix} A_i \\ F_j \end{pmatrix} \to \begin{pmatrix} F_1 \\ F_{j+1} \end{pmatrix} \to \ldots \begin{pmatrix} F_k \\ R_1 \end{pmatrix} \to \ldots \begin{pmatrix} R_1 \\ R_1 \end{pmatrix}\,,$$

— a cell in F_i meets a cell in F_j where $i < j$. Then

$$\begin{pmatrix} F_i \\ F_j \end{pmatrix} \to \begin{pmatrix} F_{i+1} \\ F_{j+1} \end{pmatrix} \to \dots \begin{pmatrix} F_k \\ R_1 \end{pmatrix} \to \dots \begin{pmatrix} R_1 \\ R_1 \end{pmatrix} .$$

Thus, in the long-time limit, the interactions between any two FRA cells always lead to the phase difference between cells equal to zero. Let us call such common oscillation as *marching FRA cells*. The duration of the system period is T as in the case of the free cellular evolution. However, due to the process of accepting the same oscillation, the cells evolve with the same oscillatory phase.

The solution as the pattern of the marching FRA cells is distinct from the set of possible results obtained when the FRA system evolves without the rule (3). In the latter case, when evolution is driven only by rules (1) and (2), the entrainment leads to states where difference between oscillatory phases of neighboring cells is equal to $+1$ or -1. Moreover, at special conditions the mutual entrainment between cells is observed what provides the sustained stable evolution with the shortest possible period T^*. The solution with marching FRA cells exists, however this solution is unstable, hence unobservable in simulations, see [16].

Def. of a FRA network:
A FRA network of density d consists of $N = L \times L$ FRA cells located in vertices of 2-dimensional square lattice of linear size L, where any two cells in any of Moore neighborhoods are connected with probability d. The boundary conditions of a system are open.

Let us recall that the Moore neighborhood comprises the eight cells surrounding a central cell and the central cell itself. It is worth to note that in order to establish a FRA network with 4–6 neighbors, d should be between 0.50 and 0.75.

Def. of intercellular interactions:
A cell being in any of the *Active* states A_i executes the rule (2) only if more than N_{F} of its nearest neighbors are in any of the *Firing* states F_i. We denote this threshold $F > N_{\mathrm{F}}$.
A cell being in any of *Refractory* states R_i executes rule (3) if more than N_{R} of its nearest neighbors are in any of the *Firing* states F_i. We denote this threshold $R > N_{\mathrm{R}}$.

Thus, interactions are driven by two parameters N_{F} and N_{R}. By changing the value of parameters N_{F} and N_{R} we can influence the sensitivity of intercellular interaction.

4. Results

We concentrate on results obtained from the FRA system where durations of states are $f = 10$, $r = 11$, $a = 19$. The values of f, r, a are chosen to approximate the relations between durations of particular states that occur in natural nodal cells located at the center of the sinus node, compare with Fig. 1 and see [12].

In Fig. 2 we show snapshots taken from typical states obtained when influence of rule (3) is strongly limited. Specifically, we assume that at least five nearest neighbors have to be in any of *Firing* states to influence a cell being in the *Refractory* state.

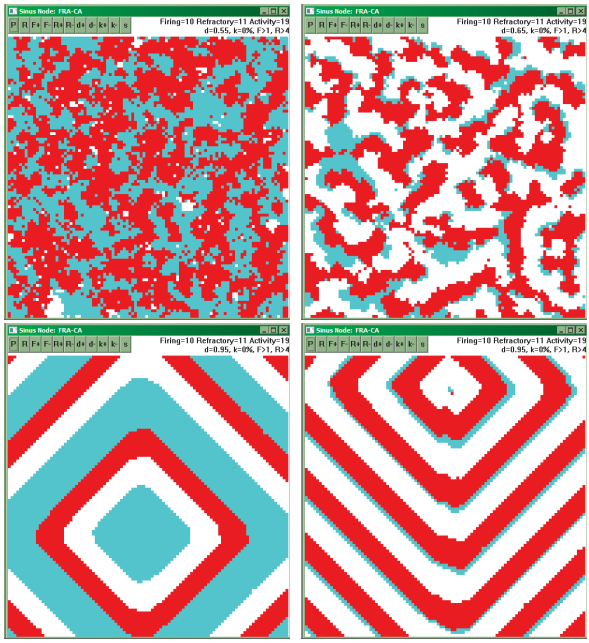

Fig. 2. Typical stationary states of the system if density of intercellular connection changes from $d = 0.55$ (top-left figure), $d = 0.65$ (top-right figure) to $d = 0.95$ (bottom figures) for $F > 1$ and $R > 4$. Black (red) color denotes cells in F_i states, white color marks cells in R_i states and gray (pale blue) color is used to denote cells in A_i states.

It appears that if rule (2) dominates and density d is low then the state consists of many small-size clusters of cells in which cells perform the synchronized evolution, see top-left panel in Fig. 2. If the connectivity between cells increases, a transition is observed from configurations with patterns without visible waves, to fractured, spiral-like waves. In the case when $F > 1$ and $R > 4$, this transition takes place at $d \approx 0.65$. If density d is

large, here, close to 1, then a small number (often one) of a strong concentric wave emerges. In this limit two types of states are observed. The first type has a property that each cell evolves according to the intrinsic cycle but, due to interactions, all cells have oscillatory phases adjusted — phases of nearest neighboring cells differ by ± 1. Because of this phase arrangement, we can observe configurations as moving stripes that are as wide as the duration of the corresponding phase. The other type of solution is shown in Fig. 2 bottom-right. Here all cells evolve with the shortest cycle T^*. This is possible due to the existence of a set of mutually entrained cells that are the source of the fast oscillation. Then the oscillatory phase adjustment among all neighboring cells allows to propagate this fast oscillation outside the source.

The description of configurations could become more clear if we apply the predator-prey concept on the cluster level [17].

Let the collection of cells within the *Firing* states be seen as the predator (black/red), while the excitable cells — cells in the *Active* states (gray/pale blue), play the role of the prey. The idea is that cells in the *Firing* states (*i.e.*, the predator cells) are all capable of exciting ("eating") cells in the *Active* states (*i.e.*, the prey cells). Without the prey around, predator cells move to the *Refractory* state (white). Following a *Refractory* period, dead cells will regenerate and become prey cells.

Let us apply the concept of predator-prey to the states shown in Fig. 2. We see that the areas of the predator have elongated and usually curved shapes. The predator clusters are bordered with homogeneous regions of the preys at the outer side with respect to the curvature of the cluster. On the opposite side of the predator cluster there are cells in the *Refractory* states only. Therefore the cluster evolution can be described as the expansion of the predator from some centers of spirals to the borders of the FRA network.

In Fig. 3 we present configurations obtained when cells in the *Refractory* states are strongly sensitive to neighbors being in the *Firing* states. Namely, we assume that at least 5 nearest neighbors have to be in any of *Firing* states to influence a cell that is in any of *Active* states while only two neighbors in *Firing* states are sufficient to elongate the *Refractory* phase of a cell.

As we expect the solution with marching FRA cells occurs rather frequently. However, the emergence of large waves of the predator takes place too. In the case of $F > 4$ and $R > 1$ it appears at density $d = 0.65$, see top-right panel in Fig. 3. However, the clusters of the preys are located inside the predator area. Therefore, the predator chasing after the preys looks like collapsing from the borders of the system to some region in the center. The solution with collapsing spiral is not the only solution observable at $d = 0.65$ but it emerges with probability around 0.5.

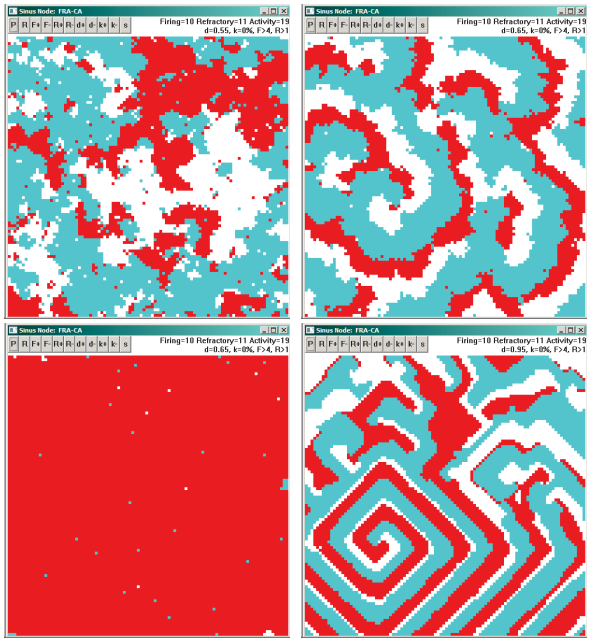

Fig. 3. Typical stationary states of the system if density of intercellular connection changes from $d = 0.55$ (top-left figure) by $d = 0.65$ (top-right and bottom-left figures) to $d = 0.95$ (bottom-right figure) for $F > 4$ and $R > 1$. Black (red) color denotes cells in F_i states, white color marks cells in R_i states and gray (pale blue) color denotes cells in A_i states.

When the density of connections is large enough then after a very long evolution (more than 20000 time steps) a strong collapsing spiral is always obtained, see bottom-right panel in Fig. 3. The period most often found is $T + 1$. The extra step is due to the persistent elongation of the *Refractory* state when a cell is at the edge of the predator area.

Fig. 4 emphasizes the difference between the two wave solutions discussed above. We show there the strong "perfect" spiral waves of each type: expanding (left plot) and collapsing (right plot). Such strong wave forms were observed at different densities and for many values of F and R. Therefore, by switching values of F and R and changing the density d of intercellular connections we searched for conditions at which expanding or collapsing spiral-patterns appear in the FRA network. Specifically, in computer experiments, we observed the stationary states and qualified them according to the shape of the predator, *i.e.*, by properties of the *Firing* state patterns.

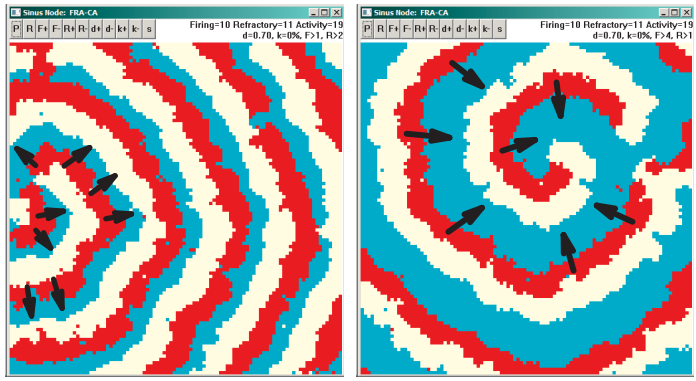

Fig. 4. Configurations with two types of states: expanding excitation wave front (predators) from some center to the borders (left), and collapsing excitation wave front from the borders to some center part (right). Arrows additionally point at direction of the front of excitation.

At first, the stationary states were split into configurations without any signs of pattern structure (*e.g.*, states like top-left in Figs. 2 and 3) and others. Then, the states of the second group were classified with respect to the presence of expanding or collapsing spirals. Usually these events were interwoven by the state with all cells marching. Moreover, in some case we observed the expanding or collapsing wave pattern living only in some bounded part of the plane. The situations where the marching cells solution coexisted with the spiral solution, we qualified as a mixture of the march and the corresponding spiral.

Tables I and II collect results of our simulation experiments found after at least 50 runs for each case. The density values, which are not explicitly shown in the tables, correspond to events where either we always did not obtain any signs of pattern structure (case of small densities), or the solution was always the marching cells (case of large densities).

The geometrical relations can be though as imitating temperature effects present in a thermodynamic system. Namely, the small density of connections can be interpreted as the high temperature regime. FRA cells live independently of each other what leads to rather random patterns of the predator regardless of the interaction sensitivity. The opposite case, when all 8 possible intercellular connections are established, corresponds to the frozen structure. If interactions affecting the *Refractory* phase strongly dominate over interactions changing the *Active* phase (*e.g.*, $F > 4, R > 1$) then the complex pattern with the collapsing spiral emerges. If the change in the *Active* phase is definitely more sensitive than in the *Refractory* phase (*e.g.*, $F > 1, R > 4$), then always the expanding spiral occurs. However,

in all cases between, the solution with all cells marching appears as the only solution or very probable solution. The transition between these limit solutions goes by patterns with either collapsing or expanding wave shape.

TABLE I

Probability to observe the stationary state in FRA system as a given pattern, for various values of interaction parameters F and R and density d of intercellular connections — part I.

d density	spiral of type: $\rightarrow\leftarrow$	$\leftarrow\rightarrow$	mixed state: $0+\ \rightarrow\leftarrow$	$0+\ \leftarrow\rightarrow$	march
case: $F > 0$, $R > 0$					
0.30		0.73		0.23	0.04
0.35		0.29		0.21	0.50
0.40		0.20		0.12	0.68
0.45		0.18			0.82
0.50					1.0
case: $F > 1$, $R > 0$					
0.45	1.00				
0.50	0.64				0.36
0.55	0.63				0.38
0.60	0.29				0.71
0.65	0.06		0.06		0.88
0.70	0.05				0.95
0.75					1.00
case: $F > 0$, $R > 1$					
0.60		1.00			
0.65		0.79		0.21	
0.70		0.61		0.34	0.05
0.75		0.24		0.48	0.28
0.80				0.43	0.57
0.85				0.20	0.80
0.90				0.07	0.93
0.95					1.00
case: $F > 2$, $R > 0$					
0.45	1.00				
0.50	0.90				0.10
0.55	0.68				0.32
0.60	0.24				0.76
0.65					1.00

Notation used in the table headings:
$\rightarrow\leftarrow$ = collapsing spiral; $\leftarrow\rightarrow$ = expanding spiral; $0+\ \rightarrow\leftarrow$ = march coexisting with collapsing spiral; $0+\ \leftarrow\rightarrow$ = march coexisting with expanding spiral.

TABLE II

Probability to observe the stationary state in FRA system as a given pattern — part II.

d density	spiral of type: $\rightarrow\leftarrow$	$\leftarrow\rightarrow$	mixed state: $0+\ \rightarrow\leftarrow$	$0+\ \leftarrow\rightarrow$	march
case: $F > 1$, $R > 1$					
0.50					
0.55			0.15	0.23	0.62
0.60			0.22	0.21	0.57
0.65	0.04	0.15	0.29	0.21	0.32
0.70		0.14	0.08	0.04	0.74
0.75		0.13		0.07	0.80
0.80		0.06			0.95
0.85					1.00
case: $F > 1$, $R > 2$					
0.55		0.06			0.94
0.60		0.03		0.97	
0.65		0.82		0.17	0.02
0.70		0.78		0.14	0.08
0.75		0.67			0.33
0.80		0.43		0.53	0.04
0.85		0.08	0.13	0.22	0.57
0.90			0.10	0.13	0.77
case: $F > 2$, $R > 1$					
0.60					1.00
0.65	0.05		0.02		0.93
0.70					1.00
0.75	0.03				0.97
0.80	0.07				0.93
0.85					1.00
0.90	0.15				0.85
0.95	0.08	0.20			0.72
1.00		0.29			0.71

Notation as in Table I.

5. Discussion and conclusions

The FRA system has appeared extremely sensitive to the topological parameters such as strength of interactions measured by thresholds F and R and density d of intercellular connections. At densities $0.50 < d < 0.75$ the system exhibits the largest variety of possible solutions. Specifically, if $F > 1$, $R > 1$ and $d = 0.65$ then all types of stationary states were

observable. Let us recall that this density closely corresponds to the density found in the canine sinoatrial node. Moreover, it is known that the phase sensitivity of a pacemaker cell is more effective in shortening the cellular cycle, and that the overall velocity of the impulse propagation is lower in the sinus node tissue when compared to the atrial tissue [13]. In the FRA model these properties could be revealed by higher than 0 values of the thresholds F and R and with the threshold F smaller than the threshold R. In our opinion, $F > 1$ and $R > 2$ restore the real system properties in the best way. Going further from the above described correspondence, we should ask whether the other properties observed in the model could be related to some events encountered in the real pacemakers.

The interesting response could be found from analysis of the phenomenon known as hyperkalemia — high potassium level in blood. Hyperkalemia is a common clinical condition that can induce deadly cardiac arrhythmias [4,1]. The relation between the FRA model and hyperkalemia can be routed as follows. There are many types of ion channels (mainly to transport ions of sodium, potassium and calcium) that are responsible for the slow diastolic depolarization phase which in the FRA model coincides with the *Active* phase. But only potassium channels operate during the properly functioning of the repolarization phase, thereby increasing the outward directed hyperpolarizing K^+ currents [13]. It is known that when the serum potassium level is elevated to $5.78 \pm 0.96\,\mathrm{mEq/L}$, the sinus node recovery time — the time needed for completing the repolarization, is significantly prolonged [4] what decreases the action rate of the sinus node. The *Refractory* phase in the FRA model corresponds to the repolarization of the cellular membrane. If we suppose that high potassium level decreases threshold for intercellular coupling in the *Refractory* phase, *e.g.* moves $R > 2 \to R > 1$, then the FRA model could provide an explanation for the observed pathological physiological facts.

REFERENCES

[1] J. Jalife *et al.*, *Basic Cardiac Electrophysiology for the Clinician*, Wiley-Blackwell, 2002.

[2] D.C. Michaels, E.P. Matyas, J. Jalife, *Circ. Res.* **58**, 706 (1986).

[3] Y. Kuramoto, *Chemical Oscillations, Waves and Turbulence*, Springer, Berlin 1984; A. Pikovsky, M. Rosenblum, J. Kurths, *Synchronization: A Universal Concept in Nonlinear Science*, Cambridge University Press, Cambridge 2001; S. Strogatz, *Sync: The Emerging Science of Spontaneous Order*, Hyperion, New York 2003.

[4] R.E. Klabunde, Cardiovascular Physiology Concepts, accesible via `http://www.cvphysiology.com/Arrhythmias/A005.htm`

[5] S. Abramovich-Silvan, S. Akselrod, *Biol. Cybern.* **79**, 67 (1998).

[6] J.M. Greenberg, S.P. Hastings, *SIAM J. Appl. Math.* **34**, 515 (1978).

[7] H. Berry, N. Fatés, Robustness of the Critical Behaviour in the Stochastic Greenberg–Hastings Cellular Automaton Model, to appear in *IJUC* (2011).

[8] G. Bub, A. Shrier, L. Glass, *Phys. Rev. Lett.* **94**, 028105 (2005).

[9] D. Makowiec, *Int. J. Mod. Phys.* **C21**, 107 (2010); *Acta Phys. Pol. B Proc. Suppl.* **2**, 377 (2010).

[10] M.R. Boyett, H. Honjo, I. Kodama, *Cardiovascular Research* **47**, 658 (2000).

[11] E.E. Verheijck *et al.*, *Cardiovascular Research* **52**, 40 (2001).

[12] H. Dobrzynski, M.R. Boyett, R.H. Anderson, *Circulation* **115**, 1921 (2007).

[13] M.E. Mangoni, J. Nargeot, *Physiol. Rev.* **89**, 919 (2008).

[14] R.A. Luke, J.E. Saffitz, *J. Clin. Invest.* **87**, 1594 (1991); J.E. Saffitz, D.L. Lerner, K.A. Yamada, in: *Cardiac Elecrophysiology. From Cell to Bedside*, D.P. Zipes, J. Jalive, (Eds.), Saunders Co., Philadelphia, PA USA, 2004, pp. 181–191.

[15] E.M. Cherry, F.H. Fenton, *New J. Physics* **10**, 125016 (2008).

[16] D. Makowiec, *J. Cellular Automata* **5**, 431 (2010).

[17] N.F. Otani *et al.*, *Phys. Rev.* **E78**, 021913 (2008).